

Reference Standards, Uncertainties, and the Future of the NIST Electronic Kilogram

Presenter: Richard Steiner
NIST Stop 8112‡
Gaithersburg MD 20899-8112
301-975-4226

Paper Authors: David Newell, Joshua Schwartz, and Edwin Williams*

Abstract The National Institute of Standards and Technology (NIST) watt balance experiment recently made a new determination of Planck's constant with a relative standard uncertainty of 87×10^{-9} ($k = 1$), concurrently with an upper limit on the drift rate of the SI kilogram mass standard. This paper briefly describes the calibration work necessary to maintain several reference standards and subsystems for this experiment, and mentions several noise sources. These discussions suggest design improvements being built into the next generation electronic kilogram experiment, which will try to obtain 5×10^{-9} relative standard uncertainty in order to monitor the SI kilogram.

Background Theory and Experiment Description

The watt balance, as realized by Kibble [1], is a method to compare mechanically generated power relative to electrical power resulting in a measurement of Planck's constant h . The NIST version of this experiment is theoretically identical, but physically different [2]. It is shown schematically in Figure 1, much as it will appear inside a vacuum chamber in the future version now under construction. The original experiment took place in enclosed, thermally controlled areas open to room air. In brief, the experiment has a moving (and a fixed, in series opposition) induction coil, located at room temperature within a radial magnetic field and connected to a mass balance. The field is generated by two superconducting solenoids wired in series opposition. In the first part of the procedure, the coil is moved vertically at a velocity that generates a dc voltage. Measurements of the voltage, U , with position and time to obtain velocity, v , provide a ratio U/v dependent on the magnetic flux density. Next, current is run through the coil to create a force balancing that on a kilogram mass from Earth's gravity. Measurement of current, I , along with values for the mass, m , and gravity, g , provide a second ratio mg/I , also dependent on the flux density. Combining these ratios to eliminate the field dependence leads to Eq. 1,

$$\frac{mg/I}{U/v} = \frac{mgv}{UI} = \frac{\{mgv\}_{\text{SI}} W}{\{UI\}_{90} W_{90}} \equiv 1 \text{ in SI.} \quad (1)$$

‡ Electricity Division, Electronics and Electrical Engineering Laboratory, Technology Administration, U.S. Department of Commerce.

* Contribution of the National Institute of Standards and Technology. Not subject to copyright in the U.S.

Since this experiment compares the watt W as the SI unit of power with W_{90} in 1990 representation units of V_{90}^2 / Ω_{90} , it has become known as the watt balance.

There is no difference between methods of generating power in the SI system. However, electrical references in terms of {reference values} and units are only representations, derived from a voltage proportional to the Josephson constant $\{n / K_{J-90}\} V_{90} = \{nf / K_J\} V$, and a resistance proportional to the von Klitzing constant $\{R_{K-90} / i\} \Omega_{90} = \{R_K / i\} \Omega$, where f is frequency and n, i are quantum numbers, and K_{J-90} and R_{K-90} are the 1990 assigned constants. From the theoretical values of the constants in Eq. 2, where e is elementary charge, then combining all equations in Eq. 3

$$\{K_J^2 R_K\} = \left\{ (2e/h)^2 (h/e^2) \right\} = 4/h \quad (2)$$

$$(\{mgv\} / \{UI\}_{90}) / \{K_{J-90}^2 R_{K-90}\} = h/4. \quad (3)$$

Any difference from unity in the ratio of W/W_{90} in Eq. 1 implies from Eq. 3 that the value of h as used in the electrical constants has been incorrectly assigned. Or, for a fixed value h and a sufficiently low uncertainty over time, the SI International Prototype Kilogram (IPK) is changing. It is this idea which is now driving further development of the watt balance into an electronic method to monitor IPK.

In our previously reported results on the determination of Planck's constant, h [3,4], the uncertainty was estimated at 8.7×10^{-8} (All uncertainties are relative standard uncertainties with $k = 1$, unless otherwise specified.). This is a factor of 2 smaller than reported by Kibble [5] and in comparison with his result, gives an upper limit for the drift of the SI kilogram of $(1 \pm 2) \times 10^{-8}$ per year. Is it possible to find ways to improve our design enough to gain another factor of 5, in order to monitor IPK at roughly the same uncertainty as mass calibration transfers? In the next sections we try to examine this question.

Uncertainty: More Than Data Noise

The complete uncertainty budget (Table 1) indicates how well this experiment performed, and can assist in the design of the next generation. In this paper, we follow a few of the uncertainty threads for this experiment and describe the design changes underway to reduce those uncertainties. Look-

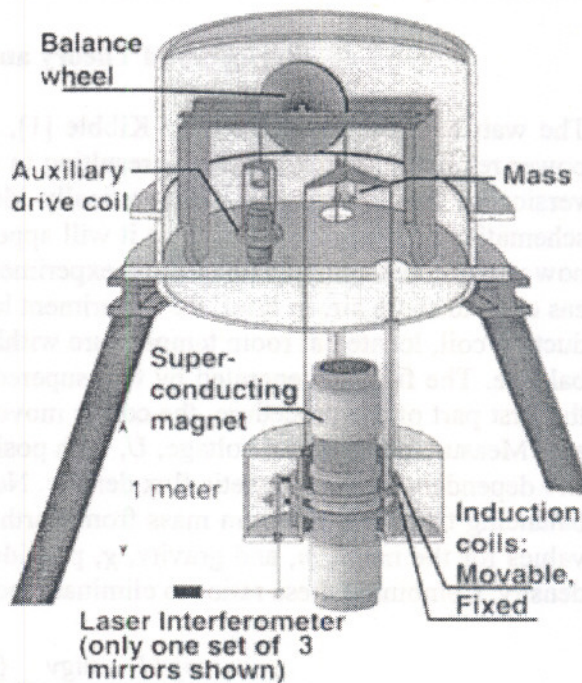


Figure 1. A schematic of the apparatus of the Watt balance. The upper vacuum chamber sits atop a tripod support, which will also suspend a liquid helium Dewar (not shown) containing the magnet.

ing at Eq. 1, the variables are dependent upon reference standards (atomic clocks, Josephson effect, etc.) that have laboratory representations with relative uncertainties at the parts in 10^9 level. But each of our measurements has a traceability path to these references with uncertainties added by each transfer. Also, each intermediate standard or instrument adds its own scatter. Part I of this section examines these transfers with several examples showing the histories of our reference calibrations. The next parts tackle more complicated analyses, where uncertainty in the measurements is from multiple instruments (Part II) in systems measuring gravity acceleration and the environmental information for calculating the air refractive index and buoyancy. Part III looks at components where the uncertainty is not a function of calibrations but is the result of noise sources external, or internal, to the watt balance system. The examples chosen are EMI, acoustic vibrations, and material deformations in the balance knife-edge.

Part I: "Simple" Reference Standards

For good reason, most fundamental constant measurements are performed in national standards laboratories. Having nearly direct access in establishing traceability to many other NIST divisions was vital, as we found that "standard references" are not always so. Of all references used, the easiest should have been the time and frequency standard. However, the NIST standard is in Boulder, and Gaithersburg no longer has a distributed frequency network, so we used an ovenized crystal source to provide a distributed standard frequency to the instruments requiring such. Drifting by a few parts in 10^9 per month, the crystal was periodically tuned to within a few parts

Table 1. The uncertainty budget for the 1998 determination of Planck's constant. Values are for $k = 1$.

Standard Uncertainty Source	nW/W
Reference Units	
Voltage	30
Mass	20
Resistance	8
Length	5
Frequency	5
Gravity	7
External Effects	
Refractive index	43
Mass buoyancy	23
Alignments	40
Leakage resistance	20
Magnetic flux z-profile fit	20
Knife edge Hysteresis	20
RF noise offsets	10
RSS sub total	82
Statistical Type A	30
Combined standard uncertainty	87

in 10^{10} against a rubidium standard, available as a part of a gravimeter system. However, the rubidium standard was eventually found to have a fractional 2.3×10^{-9} offset. Fortunately, the simple purchase of a GPS frequency receiver will provide a much better frequency reference for the future.

Still quite simple is the calibration of a He-Ne laser frequency for use as the interferometry length standard. Figure 2 shows the record of wavelength checks of our laser against an iodine-stabilized laser. The He-Ne laser does drift a bit and has some noise, but more frequent checks and better room temperature control should improve this length standard.

The current I is measured by the voltage drop across a 100Ω resistance standard. Getting progressively more complicated, Figure 3 shows the history of the two resistors in the experiment, as they were periodically transferred to the NIST Resistance Group for calibration against the 1Ω standard bank, which traces to a Quantum Hall Effect (QHE) system via a 100Ω resistor set. Resistor R1211 was chosen for its low-noise characteristics, even though R1208 had less drift and

transfer at 1.018 V to establish traceability to a Josephson array voltage standard, which has its own uncertainty of 0.005 parts in 10^6 . All signal voltages were measured against a low-noise voltage source. Consisting of a Hg battery-stabilized current source and a resistor, its peak-to-peak noise over minutes was less than 10 nV, but the drift was typically 500 nV/h. This in turn was calibrated hourly against a Zener reference. Both of these were kept in the experiment room where temperature was generally controlled to $(25 \pm 0.05)^\circ\text{C}$. The Josephson volt system was set up in the same building to calibrate the Zener reference daily. Figure 5 compares the history of two Zener references used in the later months of the experiment. The data includes corrections for thermal emfs in the 10 m leads extending into the elevated temperature of the Zener area. The second Zener is clearly quieter but was suffering an extended nonlinear drift, a "burn-in" from a recent repair. For the next generation experiment, a programmable Josephson array will be available. A prototype system was tested in Oct. 97, successfully measuring each voltage source, including noisy signals from the induction coil itself. By reducing the number of transfers and thermal emf links, an uncertainty closer to the base uncertainty of the Josephson system itself will apply.

Part II: Systems within Systems

Quite different from the direct use of reference standards in the main balance system, there are three essential variables that result from their own independent systems. The acceleration of gravity, g , is determined by a commercial gravimeter, which records the trajectory of a corner cube dropped in a vacuum. The g value (correcting for tides) for our locality is virtually constant, in contrast with the refractive index and the mass buoyancy in air, which are continually calculated from measurements of temperature, pressure, relative humidity, CO_2 concentration, and other air constituents.

Since it is simpler to analyze, let's examine the gravimeter system first. The manufacturer rechecked the iodine-stabilized laser length standard and rubidium frequency standard during the summer of 1997. (The gravimeter also needs to measure atmospheric pressure, to estimate the air mass overhead.) The system has an uncertainty specification of 2×10^{-9} . Figure 6 shows a typical measurement run. The graph clearly shows that tidal effects, calculated in software for a given location, must be subtracted from the data to obtain the local average. It is unclear whether there

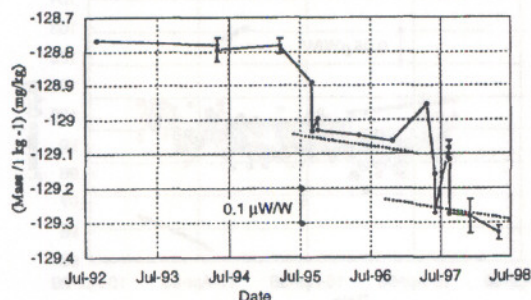


Figure 4. Calibration history of the 1 kg mass. A few error bars ($k=2$) are shown for comparing the drift with the calibrations. Dotted lines have a constant slope to compare drift rates.

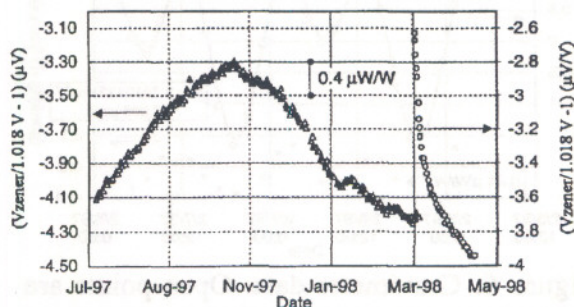


Figure 5. Calibration history of two Zener references at 1.018 V against a Josephson array volt standard.

are significant, additional diurnal effects related to tides that cannot be computed. However, the actual mass position was 4 m higher and about 5 m away from the location of the gravimeter, requiring a fractional correction of $(1.363 \pm 0.005) \times 10^{-6}$. A U.S. Geological Survey team with a gravity transfer meter measured this in Sept. 1997.

It was impossible to obtain such a low uncertainty for the calculation of the refractive index and the buoyancy corrections, about $300 \mu\text{W/W}$ and $60 \mu\text{W/W}$ respectively. Monitoring the environment parameters for these calculations [6] required a large number of sensors. The dominant parameter in both is pressure. A single sensor at the level of the mass recorded pressure for the buoyancy correction, but with the induction coil 2.6 m lower, 0.2 Pa was added for the refractive index correction. This offset was calculated and checked with a second pressure meter, which also acted as our transfer standard to the NIST Pressure Group. Four thermistors were used to measure temperatures at various locations near the interferometer paths and the mass. These were calibrated with an AC resistance bridge thermometer, which in turn was calibrated by the NIST Temperature Group. Extra effort went into controlling the temperature of the balance room and reducing gradients, especially the large ones of several degrees near the liquid helium Dewar. A relative humidity sensor was calibrated against an absolute dew-point hygrometer. A manufacturer-tested CO_2 meter recorded an average level fraction of 400×10^{-6} in the enclosure (and that it rose significantly when people were working inside). A residual gas analyzer recorded no large concentrations of non-standard gasses, especially helium, which had given measurable offsets in several older sets of data. All these measurements and calculations were checked with a dual path interferometer, built by Fujii [7] and improved by Newell. Figure 6 shows a set of measurements agreeing with calculations to within $0.05 \mu\text{W/W}$, which was consistent with the combined uncertainty of all the sensor calibration uncertainties.

Because the refractive index is so large and uncertain, the crux of the new system design is a vacuum chamber to house the entire balance and induction coil. Our choice was to make it out of a nonmagnetic material (fiberglass) to avoid expected effects from the high magnetic field or eddy currents. Outgassing of solvents should not be a serious problem. The need to dissipate the heat from current in the coils restricts lowering the operating pressure to about 10 Pa. Maintaining a low-pressure helium atmosphere reduces the refractive index and buoyancy corrections to less than 50×10^{-9} , easing the calibration requirements of the environmental sensors accordingly. The

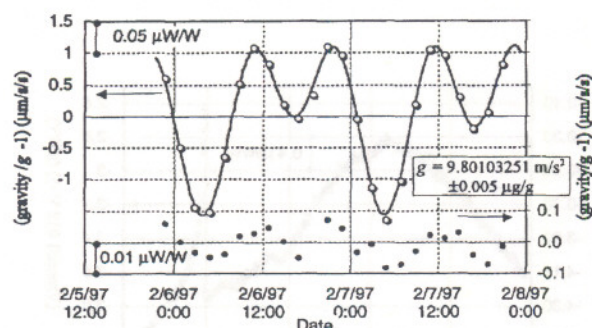


Figure 6. Gravimeter data. Open points are averages of 100 drops in 17 min, offset from the best fit value for g . The solid curve is the calculated tidal variation. Closed points are the residual deviations.

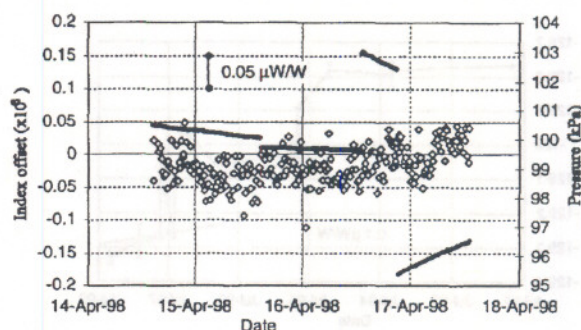


Figure 7. Refractometer data. Open points are the difference between the measured and calculated refractive index of air. Dark lines are the pressure, proportional to the index = 263×10^{-6} at 100 kPa (25 °C, 40 % RH).

gas composition will still be a consideration for the index, but surface water and dirt contamination of the mass should be greatly reduced.

Part III: There Are Noise Sources

Measurement noise, as opposed to transfer uncertainties, limits the precision for both modes of the balance. Here is a brief description of the effects of three of known noise sources and the design changes that we hope will reduce their effects. The largest noise source, if not necessarily the worst, is acoustic vibration. The building air fans generate mostly 28 Hz vibrations, and even though located some 80 m away in a separate building, the vibrations carry quite well through the earth. Also located within 100 m is the cooling tower for the NIST experimental reactor. By coincidence, the structure of the coil support assembly had a vibration mode resonance of 28 Hz. Vibrations in themselves should not be a problem, since motions relative to the fixed inductive coil with velocity v correlate with voltage U . The ratio of these variables is only a constant function of the magnetic flux density. However, there is an RLC resonance for the coils, which phase delays the 28 Hz voltages relative to the velocity. Furthermore, the floor, walls, or the coil itself could generate acoustic air waves that would register across the interferometer beam as small velocities with no corresponding voltage. As can be seen in Figure 8, the large variations due to vibration are nearly compensated in the ratio, with about 20 $\mu\text{W/W}$ p-p noise remaining.

Several design changes are intended to reduce this effect in the next generation. (1) The structure of the coil support is being stiffened to raise the resonant mode frequencies. (2) Our small laboratory building was modified to house a room with no contact to the structure of the building, including an isolated concrete floor. Although not likely to reduce the 28 Hz from the fans, it should reduce other pulsed vibrations arising from strong winds shaking the building. (3) The filter characteristics of the coil can be flattened or some digital filter matching of the velocity can be tried. (4) Ultimately, an active vibration-servo system will be installed at the base of the tripod support structure.

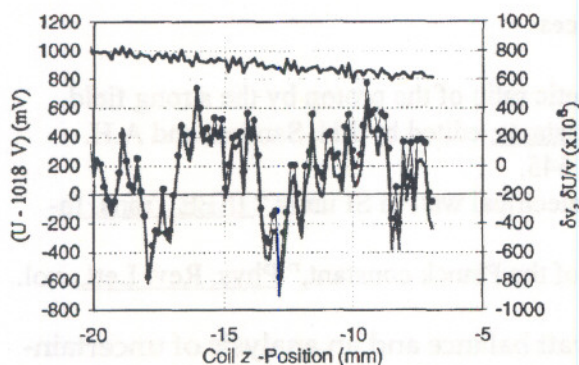


Figure 8. Velocity and voltage data. The gray line is voltage U . The closed points are velocity v relative to an average of 2 mm/s. The jagged line at top is the U/v ratio relative to an arbitrary average, where the slope is a z -dependence in the magnetic flux density.

Another noise source is EMI, mainly power-line frequencies. The series-opposition wiring of the fixed coil effectively cancels 60 Hz, but higher harmonics of 360 Hz and 480 Hz arise from slight variations in the RLC resonance of each coil. These are easily filtered with powerline integration, but can be close to the sampling frequency of some chopper-stabilized pre-amplifiers, thus causing large beat frequencies. Some EMI frequencies interfered with the signal output of the interferometer or x - y position laser detectors. The thermistors were also very sensitive. In the event of nearby lightning or strong radio transmissions, a surge in the balance servo-feedback or loss of interferometer position count could result. To reduce these effects, the new experiment room walls are lined with copper sheet (again

avoiding magnetic materials). RFI shielding tests showed at least a 30 dB reduction at 400 MHz.

Finally we mention an internal noise source, knife-edge hysteresis, possibly the worst problem for potential offsets. The balance must act like a frictionless mass balance, but also must undergo $\pm 10^\circ$ of rotation during the velocity mode. Thus a knife-edge was chosen as the pivot. Presently a Tantun-G alloy is used, in part because it has demonstrated better durability than a sapphire edge. However, for any knife edge it is known that even small rotations of 10 mrad can induce a distortion in the edge geometry. When returned to a previous balance position, this distortion produces time-dependent restoring forces. Thus, if the wheel rotates when the mass is placed on or taken off, these external balance forces do not completely cancel. Records of the rotation of the balance during mass positioning during the final two weeks showed that when the rotation was small and random, effects were minimal. But when the rotation was systematic or very large, the signal noise increased and had a definite offset. This explained deviations seen in some earlier data. To improve the balance in the next system, a completely new mass placement and servo-control will be used. The goal is to keep balance rotations during mass placement to well within 1 mrad, equivalent to restricting the mass pan within a few micrometers travel when positioning the mass. In the long term, the knife-edge will be replaced with a design using dual flexures or a flexure and vertical translation stage.

Estimating the Future

Construction of the new room inside the laboratory building began after the last data point recorded in April 1998, and was finished in October 1998. The tripod is erect, with the vacuum chambers and Dewar in place. The list of new equipment yet to be obtained, assembled, tested, and programmed includes interferometer electronics, resized induction coils, the mass mover servo-controlled system, the programmable Josephson voltage array, and a low noise voltage pre-amp. Many subsystems "just need re-assembly". Hopefully, some substantial subsystem testing *in situ* can begin late in 1999, so preliminary watt/kilogram data might be available by late 2000.

References

- [1] B.P. Kibble, "A measurement of the gyromagnetic ratio of the proton by the strong field method," Atomic Masses and Fundamental Constants, edited by J.H. Sanders and A.H. Wapstra, (Plenum, New York, 1976), vol. 5. p. 545.
- [2] P.T. Olsen, et al, "A measurement of the NBS electrical watt in SI units," IEEE Trans. Instrum. Meas., vol. 38, no. 2, 1989, p. 238-244.
- [3] E.R. Williams, et. al., "Accurate measurement of the Planck constant," Phys. Rev. Lett., vol. 81, No. 12, 21 Sep. 1998, p. 2404-2407.
- [4] R.L. Steiner, et. al, "A result from the Nist watt balance and an analysis of uncertainties", IEEE Trans. Instrum. Meas., vol. 48, No. 2, Apr. 1999.
- [5] B.P. Kibble, et. al., Metrologia, vol. 27, 1990, p. 173-192.
- [6] R. S. Davis, "Equation for the determination of the density of moist air (1981/91)," Metrologia, vol. 29, 1992, p. 67-70.
- [7] K. Fujii, "A new refractometer by combining a variable length vacuum cell and a double-pass Michelson interferometer," IEEE Trans. Instrum. Meas., vol. 46, no. 2, 1997, p. 191-195.